Wind and Structures, *Vol. 24, No. 5 (2017) 465-480*
DOI: https:// doi.org/10.12989/was.2017.24.5.465

Consistent inflow boundary conditions for modelling the neutral equilibrium atmospheric boundary layer for the SST k-ω model

Yi Yang[*1], Zhuangning Xie[1a] and Ming Gu[2b]

[1]*State Key Laboratory of Subtropical Building Science, South China University of Technology, Guangzhou 510640, China*
[2]*State Key Laboratory of Disaster Reduction in Civil Engineering, Tongji Univeristiy, Shanghai, 200092, China*

(Received April 1, 2016, Revised April 6, 2017, Accepted April 7, 2017)

Abstract. Modelling an equilibrium atmospheric boundary layer (ABL) in computational wind engineering (CWE) and relevant areas requires the boundary conditions, the turbulence model and associated constants to be consistent with each other. Among them, the inflow boundary conditions play an important role and determine whether the equations of the turbulence model are satisfied in the whole domain. In this paper, the idea of modeling an equilibrium ABL through specifying proper inflow boundary conditions is extended to the SST k-ω model, which is regarded as a better RANS model for simulating the blunt body flow than the standard k-ε model. Two new sets of inflow boundary conditions corresponding to different descriptions of the inflow velocity profiles, the logarithmic law and the power law respectively, are then theoretically proposed and numerically verified. A method of determining the undetermined constants and a set of parameter system are then given, which are suitable for the standard wind terrains defined in the wind load code. Finally, the full inflow boundary condition equations considering the scale effect are presented for the purpose of general use.

Keywords: computational fluid dynamics; computational wind engineering; self-sustainable equilibrium atmospheric boundary layer; boundary conditions; SST k-ω Model

1. Introduction

Modelling equilibrium atmospheric boundary layers (ABLs) in Computational Fluid Dynamics (CFD) is an important precondition for modelling boundary-layer related flow phenomena, such as wind effect on buildings, air pollution dispersion in urban areas, snowdrift of large-span structures, etc. Equilibrium ABLs imply horizontal homogeneity, which means that the streamwise gradients of all variables should be zero. The requirements of modelling an equilibrium ABL for the numerical investigation of wind flow have been emphasized by many researchers (Richards and Hoxey 1993, Richards *et al*. 2002, Blocken *et al*. 2007, Blocken 2014) because non-equilibrium ABL would bring large errors to numerical results. Thereby, both the guidelines for CFD prediction of wind flow in the urban environment by the COST Action 732 group (Franke *et al.*

*Corresponding author, Professor, E-mail: ctyangyi@scut.edu.cn
[a] Professor, E-mail: znxie@scut.edu.cn
[b] Professor, E-mail: minggu@mail.tongji.edu.cn

http://www.techno-press.org/?journal=was&subpage=8 ISSN: 1226-6116 (Print), 1598-6225 (Online)

2007) and the AIJ (Tominaga *et al*. 2008) emphasized the requirement to model an equilibrium ABL prior to the numerical investigation of flow around buildings.

In the earlier stage of computational wind engineering, Richards and Hoxey (1993) concluded the boundary conditions, turbulence model and associated constants must be consistent with each other in order to adequately model the atmospheric surface layer. They proposed a set of inflow boundary conditions for the standard k-ε model that satisfied the transport equations of k and ε, in which the turbulent kinetic energy kept invariant in the vertical direction. This type of inflow boundary conditions has been widely used in CFD based on the RANS method (Franke *et al*. 2007). Hargreaves and Wright (2007) discussed some of the difficulties with implementing the RH' boundary conditions, and noted that the turbulence profiles would decay if only a subset of RH' boundary conditions was adopted. Richards and Norris (2011) showed that these conditions could be directly derived by treating the onset flow as a horizontally homogeneous turbulent surface layer with the flow being driven by a shear stress at the top boundary, and the approach was extended to four RANS turbulence models within the commercial CFD code CFX. Recently, Richards and Norris (2015) proposed a pressure driven equilibrium ABL model for RANS CFD turbulence models, which can be considered as a reasonable model for the lower half of the ABL. Balogh and Parente (2015) proposed a four-parameter turbulent kinetic energy profile to better reproduce experimental measurements within the boundary layer and above the boundary layer height based on the previous works.

Blocken *et al*. (2007) focused on wall function problems and the relationship between the wind engineering roughness length and the sand grain roughness was derived. Parente *et al*. (2011a) presented a modified formulation of the RH' wall function for turbulence production to avoid the over-prediction of the turbulent kinetic energy at the wall. They proposed a method of modifying the standard k-ε turbulence model through introducing source terms in the transport equations to allow arbitrary sets of fully developed profiles at the inlet.

The problem of simulating an equilibrium boundary layer has been investigated by the authors from the viewpoint of the turbulence model itself. Based on the assumption of local equilibrium of turbulence, the solution of the k equation of the standard k-ε model was theoretically derived, and then a new set of inflow turbulence boundary conditions was proposed (Yang *et al.* 2009). The capability of these inflow boundary conditions in producing an equilibrium ABL in the standard k-ε model had been numerically verified and demonstrated. Gorlé *et al*. (2009) extended this approach to make the profiles also satisfy the momentum and dissipation equations by making two of the turbulence model constants vary with height, while the resulting non-standard turbulence model remains unproven for general wind engineering problems. The applicability of this new set of inflow boundary condition model has been validated in recent years (Gorlé *et al*. 2010, O'Sullivan *et al*. 2011, Parente *et al*. 2011a). The research of O'Sullivan *et al*. (2011)'s finding supported the authors' work. Using the suggested more general turbulence boundary profiles, the streamwise errors could be significantly reduced if a good fit between the inflow profiles and the model was used (O'Sullivan *et al*. 2011). The new boundary condition model has been adopted in some relevant simulation research (Barić *et al.* 2010, Kozmar 2011, Labovský and Jelemenský 2011, Parente *et al.* 2011b).

This paper is an extension of the authors' previous research (Yang *et al*. 2009). Some new findings and results are reported, which aim at providing a more general solution to the problem. The idea and research method, which were originally proposed based on the standard k-ε model, are now further extended to the SST k-ω model, which is regarded as a better turbulence model describing the separated flow, and two new sets of inflow boundary conditions corresponding to different descriptions of the inflow velocity, i.e., the logarithmic law and the power law respectively, are proposed for modelling the equilibrium ABL. Then a method determining the constants in the new models is proposed, and a parameter system corresponding to four typical terrains in the wind load code is given. Finally, the full equations considering the scale effect are proposed for general use purpose.

2. Equilibrium ABL model for the SST k-ω model

The k-ω based SST (Shear Stress Transport) model was developed by Menter (1994) to effectively combine the robust and accurate formulation of the k-ω model in the near-wall region with the free-stream independence of the k-ε model in the far field. A blending function is adopted to bridge these two models. The SST k-ω model takes into account the transport of the turbulent shear stress and gives highly accurate predictions of the onset and the amount of flow separation under adverse pressure gradients (Menter 1994). For this reason and relatively high efficiency in numerical solution, the two-equation SST k-ω model was adopted more frequently for the numerical simulation of bluff body flow. Yang *et al*. (2008) calculated the mean wind loads on a typical low-rise building employing the SST k-ω model and compared them with the wind tunnel test results.

The equations of the Wilcox k-ω model are multiplied by a blending function F_1, and the transformed k-ε equations are multiplied by the function $1\text{-}F_1$. Then the corresponding turbulent kinetic energy k equation and the turbulent dissipation rate ω equation are obtained to form the SST k-ω model

$$\frac{\partial \rho k}{\partial t}+\frac{\partial}{\partial x_j}\left(\rho u_j k-(\mu+\frac{\mu_t}{\sigma_k})\frac{\partial k}{\partial x_j}\right)=P_k-C_\mu \rho \omega k \tag{1}$$

$$\frac{\partial \rho \omega}{\partial t}+\frac{\partial}{\partial x_j}\left(\rho u_j \omega-(\mu+\frac{\mu_t}{\sigma_\omega})\frac{\partial \omega}{\partial x_j}\right)=\alpha\frac{\omega}{k}P_k-\beta\rho\omega^2+2(1-F_1)\frac{\rho}{\sigma_{\omega 2}\omega}\frac{\partial k}{\partial x_j}\frac{\partial \omega}{\partial x_j} \tag{2}$$

where ρ is the density of fluid, k and ω are the turbulent kinetic energy and its dissipation rate, respectively. P_k is the production of turbulent kinetic energy. The eddy viscosity in the SST k-ω model is given by

$$\mu_t=\rho\frac{k}{\omega} \tag{3}$$

Comparing the eddy viscosity in the standard k-ε model

$$\mu_t=\rho C_\mu\frac{k^2}{\varepsilon} \tag{4}$$

The following relation between ω and ε can be obtained

$$\omega=\frac{1}{C_\mu}\frac{\varepsilon}{k} \tag{5}$$

We assume a steady, incompressible and homogeneous flow. Homogeneity implies u, k and ω are invariant with the coordinates x and y, and only vary with height above ground z. Furthermore, in highly turbulent flows, $\mu_t >> \mu$. Based on the Boussinesq eddy viscosity hypothesis to estimate the Reynolds stress, P_k can be written as: $P_k = \mu_t \left(\partial u / \partial z\right)^2$. Eq. (1) then can be simplified into

$$\frac{\partial}{\partial z}\left(\frac{\mu_t}{\sigma_k}\frac{\partial k}{\partial z}\right)+\mu_t\left(\frac{\partial u}{\partial z}\right)^2 - C_\mu \rho \omega k = 0 \tag{6}$$

Substituting Eq. (3) into Eq. (6) leads to the following equation

$$\frac{1}{\sigma_k}\frac{\partial}{\partial z}\left(\frac{k}{\omega}\frac{\partial k}{\partial z}\right)+\frac{k}{\omega}\left(\frac{\partial u}{\partial z}\right)^2 - C_\mu \omega k = 0 \tag{7}$$

Assuming that the turbulence is under local equilibrium condition, i.e., the rate of production of turbulent kinetic energy is equal to the rate of dissipation: $P_k=\rho\varepsilon=\rho C_\mu k\omega$.. Combining both expressions of P_k with Eq. (3) yields

$$\omega = \frac{1}{\sqrt{C_\mu}}\frac{\partial u}{\partial z} \tag{8}$$

Substituting Eq. (8) into Eq. (7) yields

$$\frac{\sqrt{C_\mu}}{\sigma_k}\frac{\partial}{\partial z}\left(\frac{k\frac{\partial k}{\partial z}}{\frac{\partial u}{\partial z}}\right) = 0 \tag{9}$$

Eq. (9) can be rewritten as

$$\frac{k\cdot\frac{\partial k}{\partial z}}{\frac{\partial u}{\partial z}} = const. \tag{10}$$

2.1 "Log-law" type equilibrium inflow boundary conditions

We assume that the mean velocity profile can be represented by the logarithmic law

$$u = \frac{u_*}{\kappa}\ln\left(\frac{z+z_0}{z_0}\right) \tag{11}$$

where u_* is the friction velocity, κ is the von Karman constant and z_0 is the aerodynamic roughness length. Then the solution of Eq. (10) can be expressed in the following form after a simple linear transformation is introduced (Yang *et al*. 2009)

$$k = \frac{u_*^2}{\sqrt{C_\mu}}\sqrt{C_1\cdot\ln\left(\frac{z+z_0}{z_0}\right)+C_2} \tag{12}$$

In Eq. (12), C_1 and C_2 are two undetermined constants that describe the inflow turbulence level, and they could be determined by employing numerical fitting of the experimental data. Eq. (12) shows that k is a nonlinear function of the height above ground z, and the form of Eq. (12) ensures the k is positive.

In the above derivation, the analytical solution to the k transport equation (Eq. (1)) is obtained. The ω transport equation (Eq. (2)), on the other hand, is a complex nonlinear partial differential equation, for which no closed-form analytical solution can be obtained directly. If the solution to the k transport equation also (approximately) satisfies the transport equation for ω (Eq. (2)), then it would be the (approximate) solution of the complete turbulence model equations. This important supposition had been numerically verified by previous work for the k-ε model (Yang *et al*. 2009). The numerical verification in the next Section 3 will exhibit that Eq. (12) is approximately satisfied with the ω equation simultaneously, therefore, it becomes the approximate solution to the complete turbulence model equations.

Next, considering the relationships of ω with u and ε in Eqs. (8) and (5), a similar form for ω and ε could be suggested as

$$\omega = \frac{u_*}{\kappa\sqrt{C_\mu}}\frac{1}{z+z_0} \tag{13}$$

$$\varepsilon = \frac{{u_*}^3}{\kappa(z+z_0)}\sqrt{C_1\ln(\frac{z+z_0}{z_0})+C_2} \tag{14}$$

Modelling an equilibrium boundary layer in CFD requires that the inflow boundary conditions should satisfy the turbulence model equations (Yang *et al*. 2009). Based on this viewpoint, the new set of the inflow boundary conditions for modelling an equilibrium ABL with the SST k-ω model could then be proposed through the above approximate solutions to the turbulence model equations (Eqs. (11), (12) and (13) or (14)). For the logarithmic law of the velocity profile being adopted, it is referred to as “Log-law” type inflow boundary conditions hereafter.

2.2 “Power-law” type equilibrium inflow boundary conditions

Besides the logarithmic law, the mean velocity profile u could also be expressed by the power law as Eq. (15) (Davenport 1967), which is often adopted in the wind codes, such as the Load Code for the Design of Building Structures of China.

$$u = u_r(\frac{z}{z_r})^{\alpha_i} \tag{15}$$

where z_r is the reference height, u_r is the mean velocity at the reference height z_r and α_i is the power law exponent describing the corresponding terrain category.

If the power law of the mean velocity is employed, the theoretical solution to the Eq. (10) can be expressed in the following form

$$k = \sqrt{D_1 z^{\alpha_i} + D_2} \tag{16}$$

where D_1 and D_2 are two undetermined constants describing different inflow turbulence level, which are similar to C_1 and C_2 in Eq. (12). The determination of their values needs numerical fitting of the experimental data.

Considering the relationships of ω with u and ε in Eqs. (8) and (5), the similar equations for ω and ε could be obtained

$$\omega = \frac{\alpha_i}{\sqrt{C_\mu}} \frac{u}{z} \tag{17}$$

$$\varepsilon = \alpha_i C_\mu^{\frac{1}{2}} \frac{u}{z} \sqrt{D_1 z^{\alpha_i} + D_2} \tag{18}$$

where u is the mean velocity profile, $u = u_r (z / z_r)^{\alpha_i}$.

Similarly, another set of inflow boundary conditions for modelling the equilibrium ABL with the SST k-ω model, expressed as Eqs. (15), (16) and Eq. (17) or Eq.(18), is obtained. For the power law of the velocity profile being employed, it is referred to as “Power-law” type inflow boundary conditions hereafter.

Comparing above two sets of equilibrium inflow boundary conditions, i.e., the “Log-law” type and the “Power-law” type respectively, it is found that the forms of k expression are very similar, while the expressions of the ω or ε are slightly different. The “Power-law” type includes an extra variable mean velocity “u”.

3. Verification of the new equilibrium ABL model

In this section, the performances of the two types of inflow turbulence boundary conditions are demonstrated by numerically reproducing the neutral ABL flows of wind terrain categories B defined in the Load Code for the Design of Building Structures of China. The corresponding power law exponent of terrain categories, α, is 0.15, as given in Table 1.

3.1 Fitted profiles of inflow boundary conditions

The experimental data of a wind tunnel test was adopted here as the source data of the inflow boundary conditions for the numerical model. The experiment was carried out in the TJ-1 Wind Tunnel in Tongji University. The test section of the TJ-1 Wind Tunnel is 12 m long, 1.8 m wide and 1.8 m high, and the wind velocity ranges from 1.0 to 30.0 m/s. The profiles of the mean wind velocity u, and the along-wind turbulent intensity I_u, were measured at the end of the 12 m long test section.

Fig. 1 illustrates the mean velocity and TKE (turbulent kinetic energy) profiles of the wind tunnel test data and their fitted curves, respectively. The fitted curves of mean velocity u in Fig. 1 (a) are described as: $u^* = 0.511$ m/s, $\kappa = 0.42$ and $z_0 = 2.25 * 10^{-4}$ m (Here z_0 is given based on the wind tunnel test scale) with the Log-law Eq. (11); and u_r=9.3 m/s, z_r=0.47 m, α=0.16 with the Power-law Eq. (15).

The experimental data of TKE and their fitted curves are illustrated in Fig. 1(b). The four undetermined parameters are obtained through the least square approximation. Their values are taken as: $C_1 = -0.17$ and $C_2 = 1.62$ for the Log-law model and D_1=-3.02 $m^{3.84}$ and D_2= 3.51m^4/s^4

for the Power-law model. Though the numerical fitting of TKE profile in Fig. 1(b) is not as good as the one of u profile in Fig. 1(a) (It is partly attributed to the unavailability of more accurate experimental data of TKE. Only the along-wind turbulent intensity I_u was measured. Therefore, an assumption of $k=0.9*(u*I_u)^2$ was made to estimate the TKE profile.), however, it should be noted that the fitted curves based on Eqs. (12) and (16) provide a much closer agreement with the experimental data than the constant k profile which was suggested by Richards and Hoxey (1993). The discrepancy between the wind tunnel data and fitted curves will be reduced greatly if wind tunnel test data of the turbulent intensities at three directions, I_u, I_v and I_w are available (here only I_u was measured and the ratios of I_v/I_u and I_w/I_u were supposed to estimate the TKE). The numerical verification work below will not be affected by the numerical fitting errors.

3.2 Computational model

A series of 3D numerical simulations in an empty domain without any obstacles is carried out to verify the capability of the present two types of inflow turbulence boundary conditions for modelling an equilibrium ABL.

All aspects of the numerical model, including the computational domain, the mesh arrangement and all the parameters, are kept exactly the same with the previous study (Yang *et al*. 2009) for the consistency of the research. Here it is briefly introduced as below.

The size of the computational domain is L*B*H=12 m*1.8 m*1.8 m, which is consistent with the section of the wind tunnel test. The height of the first mesh layer above the ground zmin is set as 0.01 m, and the vertical growing factor of mesh points is set as 1.06. The mesh sizes in both horizontal and lateral directions are set as 0.1 m uniformly. This gives a total amount of cells of 90,720. This type of mesh arrangement model is called basic mesh model and denoted as “mesh-b” hereafter. The simulations are performed with the commercial CFD code ANSYS Fluent v. 14.5.

The boundary conditions for the computation models are listed in Table 1, in which the inflow boundary conditions for the SST k-ω model take the Eqs. (11)-(13) of “Log-law” type and Eqs. (15)-(17) of “Power-law” type respectively, and they are defined through User-defined Functions provided by Fluent. The ground boundary is modeled as a rough wall. The two parameters of the rough wall model, i.e., the roughness height KS and roughness constant CS, are determined according to the relationship between the roughness height K_S and the roughness length z_0 proposed by Blocken *et al*. (2007) as given in Table 1. The upper face of the computational domain is modeled with the free slip boundary condition.

According to the authors’ previous research, both the numerical simulation of the ABL itself and the bluff body flows immersed in ABL would be heavily influenced by the values of the turbulence parameters (Yang *et al*. 2008, 2009). Therefore, the turbulence parameters in the SST k-ω model are needed to change to be consistent with the turbulence characteristics, which could be referred to Yang *et al*. (2008). Here the turbulence parameter C_μ takes the value of 0.028 and the parameters of the inner layer Wilcox $k-\omega$ model are given as: $\alpha_1 = 0.413$, $\beta_1 = 0.0333$, $\sigma_{k1} = 1.176$ and $\sigma_{\omega 1} = 2$; and those of the outer layer $k-\varepsilon$ model are given as $\alpha_2 = 0.20$, $\beta_2 = 0.0368$, $\sigma_{k2} = 1.0$ and $\sigma_{\omega 2} = 1.168$.

The computational settings include the SIMPLEC algorithm for the pressure-velocity coupling, the QUICK scheme for the convective terms, and the central differencing scheme for the diffusion terms in the momentum and turbulence model equations. The flow field is initialized by using the values set for the inlet boundary conditions. The convergence criteria of the scaled residuals for all the variables and the continuity equation are set as 10^{-6}, and when the solutions of all the variables except for the continuity equation are converged (the scaled residual of the continuity equation reached 10^{-4} at that time and kept unchanged), additional iterations are performed until the scaled residuals of all the variables and continuity equation show no further decrease.

Table 1 Boundary conditions of computation model

Location		Boundary condition	
Inflow boundary	Velocity u and k, ω	"Log-law" type: $u=\frac{u_*}{\kappa}\ln(\frac{z+z_0}{z_0})$, $v=0$, $w=0$; $k=\frac{u_*^2}{\sqrt{C_\mu}}\sqrt{C_1\cdot\ln(\frac{z+z_0}{z_0})+C_2}$, $\omega=\frac{u_*}{\kappa\sqrt{C_\mu}}\frac{1}{z+z_0}$; in which u_*=0.511 m/s, C_1=-0.17, C_2=1.62 and z_0=0.000225 m	"Power-law" type: $u=u_r(\frac{z}{z_r})^{\alpha_i}$, $v=0$, $w=0$; $k=\sqrt{D_1 z^{\alpha_i}+D_2}$, $\omega=\frac{\alpha_i}{\sqrt{C_\mu}}\frac{u}{z}$; in which u_r=9.3 m/s, z_r=0.47 m, α=0.16, D_1=-3.02 $m^{3.84}$ and D_2= 3.51m^4/s^4.
Downstream boundary	Outflow	$\frac{\partial}{\partial x}(u,v,w,k,\omega)=0$	
Upper face of computational domain	Free slip	$w=0$, $\frac{\partial}{\partial z}(u,v,k,\omega)=0$	
Side faces of computational domain	Free slip	$v=0$, $\frac{\partial}{\partial z}(u,w,k,\omega)=0$	
Ground surface boundary	Wall	Rough wall modification with roughness height K_S=0.0025 m and roughness constant C_S=0.75.	

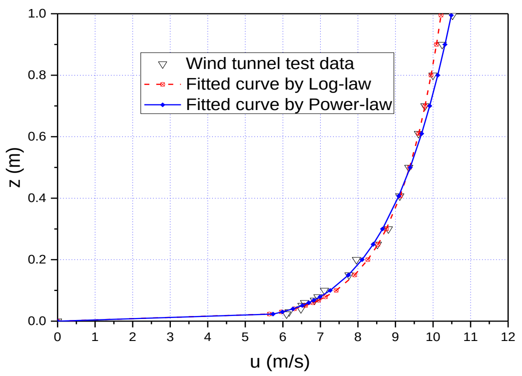

(a) Mean velocity profiles

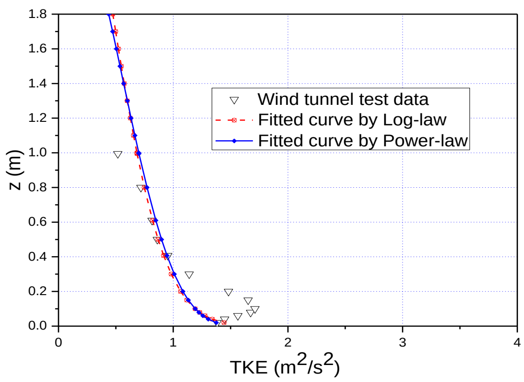

(b) TKE profiles

Fig. 1 Wind tunnel test profiles and its fitted curves

3.3 Numerical results

3.3.1 Numerical results of basic model

Figs. 2 and 3 illustrate the numerical results of the basic mesh model. Fig. 2 gives the comparisons of velocity, u, and turbulent kinetic energy, TKE, and specific dissipation rate, ω profiles at inlet and outlet under the Log-law and the Power-law inflow boundary conditions. Fig. 3 exhibits the contours of u, TKE and ω under two inflow boundary conditions on the longitudinal centre plane to get a whole picture of the numerical results.

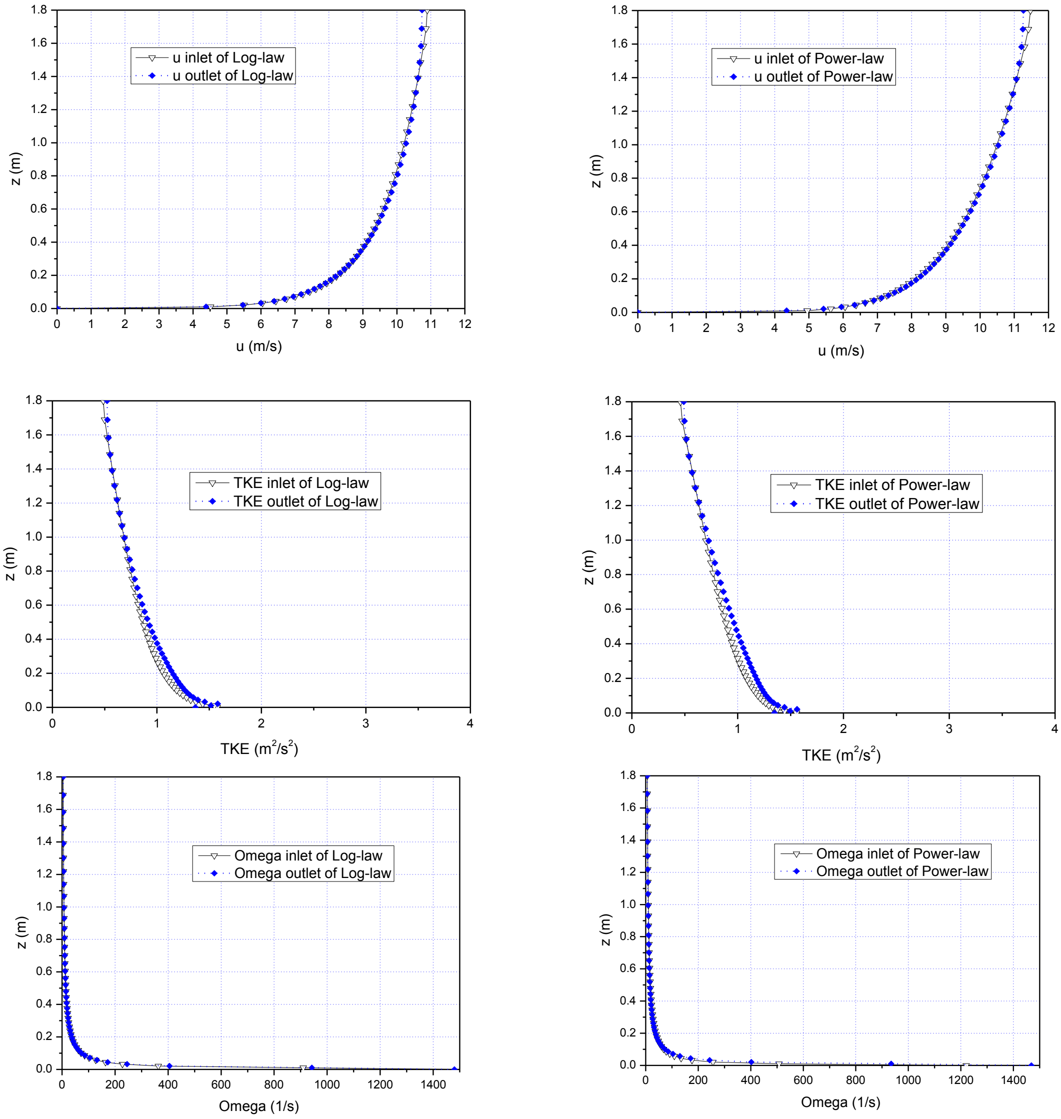

(a) Log-law (b) Power-law

Fig. 2 Comparisons of u, TKE and Omega profiles at inlet and outlet under Log-law and Power-law inflow boundary conditions

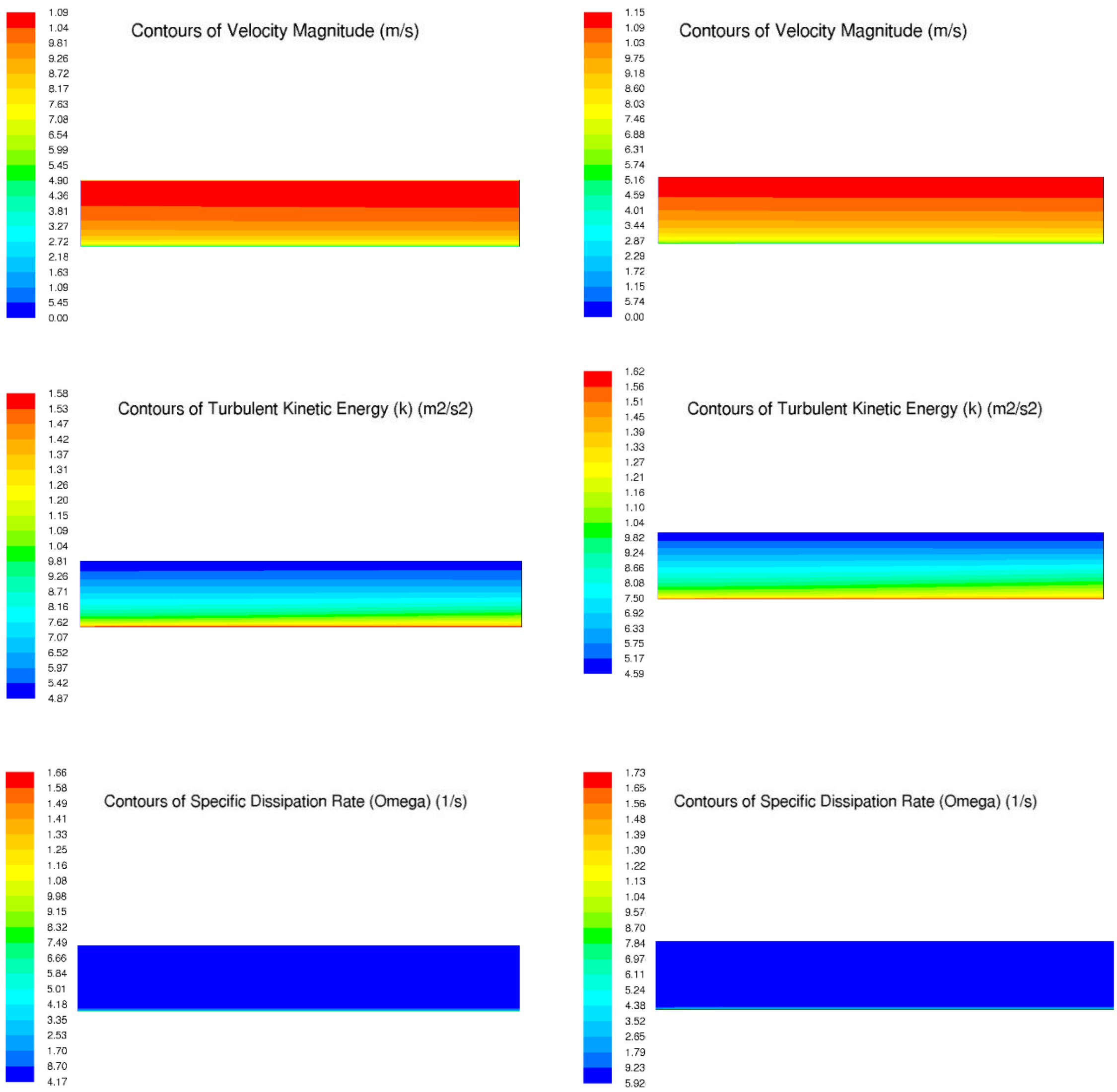

(a) Log-law (b) Power-law

Fig. 3 Contours of u, TKE and Omega under Log-law and Power-law inflow boundary conditions on longitudinal centre plane

As can be seen from the figures, under the present two inflow boundary conditions, all the profiles of the mean velocity, u, the turbulent kinetic energy, TKE and the specific dissipation rate, ω are sustained well throughout the whole domain, except for the small region near the ground and at low altitude. The errors are related to the rough wall boundary treatment and turbulence parameter setting (Blocken *et al.* 2007, Yang *et al.* 2008, 2009). Previous research

(Yang 2004) showed that the errors could be eliminated through an additional iteration, in which the resulting outlet profiles were introduced to the next iteration as the inlet boundary conditions.

3.3.2 Verification of mesh solution independence

The numerical simulations on different mesh solutions are then performed to check the requirements of mesh independence.

Two additional mesh solution cases are designed to check whether the results obtained in Section 3.3.1 are mesh-dependent. The details about the mesh arrangements of three mesh solutions (including the basic model above) are listed in Table 2. In the table, the case *Mesh-b* represents the basic calculation model described in Section 3.2; the case *Mesh-h* represents that the height of the first mesh layer from the ground, z_{min}, decreases to $1/\sqrt{2}$ of the value of the basic model, and the number of mesh nodes along the vertical direction is doubled so that it yields the double amount of mesh cells. The case *Mesh-d* represents that z_{min} increases to $\sqrt{2}$ times the value of the basic model, and the number of mesh nodes along the vertical direction is half of the basic model. Therefore, the numerical results could be investigated in a range of 2 times variation of mesh densities. All the other parameters in the additional two mesh solution models are kept exactly the same with those of the basic model. Figs. 4 and 5 illustrate the calculation results, in which the selected values ranging from 0m to 0.6m are exhibited to emphasize the results of u, k and ω near ground.

Table 2 Three mesh solutions of the numerical models

Cases	Height of the first mesh layer above the ground z_{min} (Unit: m)	Total number of mesh cells of the calculation model
Mesh-b	0.01	90,720
Mesh-h	0.007	181,440
Mesh-d	0.014	45,360

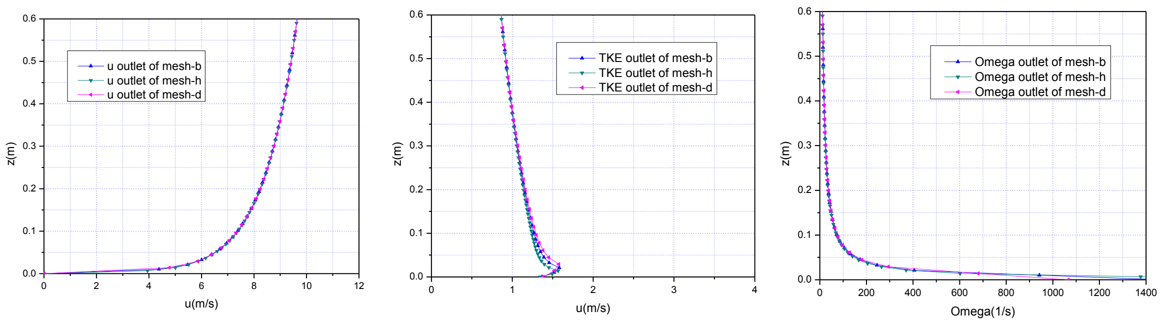

Fig.4 Comparison of the predicted outlet profiles of u, TKE and Omega on three mesh solutions under the Log-law inflow boundary conditions

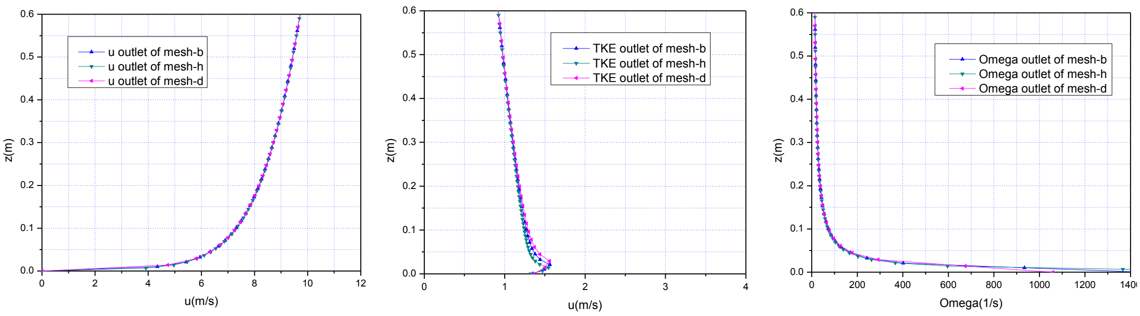

Fig. 5 Comparison of the predicted outlet profiles of u, TKE and Omega on three mesh solutions under the Power-law inflow boundary conditions

From Figs. 4 and 5, it can be seen that the numerical results of the boundary layers on three different mesh solutions (including the basic model) are very close, and all the velocity u, TKE and ω profiles of three mesh solutions can be self-sustained well. Through the comparison work, it could be concluded that the CFD numerical simulation results under present two inflow boundary conditions are independent of the mesh solutions adopted.

4. Determination of the parameters

The major difficulty of applying the proposed new inflow boundary conditions is probably to give the undetermined parameters, e.g., C_1, C_2, D_1 and D_2 etc. Here we introduce a method to determine their values, which could be served as a reasonable way to employ the proposed inflow boundary conditions if the measuring data is unavailable.

Suppose we simulate the ABL flows corresponding to four different wind terrain categories, for example, the A, B, C and D terrain which are defined in the *Load Code for the Design of Building Structures of China* (the corresponding power law exponent, α_i, has been given in Table 3). Here we could estimate k using an approximate formula as $k=0.9\,(u * I_u)^2$ (we assume $I_v \approx 0.75\, I_u$; $I_w \approx 0.5\, I_u$, which will give the coefficient 0.9), where the along-wind turbulent intensity, I_u , could be referred to *Load Code for the Design of Building Structures of China* as Eq. (19).

$$I_u = I_{10} * (z/10)^{-\alpha_i} \qquad (19)$$

where I_{10} is the turbulence intensity at the height of 10 m, and it takes 0.12, 0.14, 0.23 and 0.39 for four different terrain categories A, B, C and D respectively.

The aerodynamic roughness length z_0 is defined referred to the Eurocode 1: Actions on structures-Part 1-4: General actions-Wind actions as in Table 3, in which the terrain categories I, II, III and IV are similar to those defined in the Load Code for the Design of Building Structures of China.

None of existing wind load codes includes all the required parameters, therefore, referring to different codes while still keeping the same terrain characteristics seems a compromised but reasonable way.

Table 3 Parameters in the proposed inflow boundary conditions for four typical wind terrain categories

	"Log-law" type				"Power-law" type				
	u_* (m/s)	z_0 (m)	C_1	C_2	u_r (m/s)	z_r (m)	α_i	D_1 ($m^{4-\alpha_i}/s^4$)	D_2 (m^4/s^4)
Category A	0.6	0.01	-0.36	5.00	10	10	0.12	-5.32	14.57
Category B	0.8	0.05	-0.27	3.16	10	10	0.16	-6.33	23.75
Category C	1.2	0.3	-0.19	1.66	10	10	0.22	-8.94	53.10
Category D	2.0	1.0	-0.20	1.38	10	10	0.30	-13.65	160.74

By employing a nonlinear fitting for the TKE profile, we finally obtain a full parameter system corresponding to four different wind terrains as in Table 3, which is valid for full scale building model case only (assuming the mean wind velocity u is 10 m/s at 10 m height).

It should be noted that different methods estimating TKE or different fitting algorithm might result in different values of C_1, C_2, D_1 and D_2. Wind terrains differing from Table 3 could employ similar procedure as well.

5. Scale effect

If above parameter system in Table 3, which is valid for full scale case, is referred to the scaled model, then the "scale effect" needs to be considered carefully because the two sets of the proposed inflow boundary conditions have different expressions.

For the "Log-law" type, simply scaling all the roughness height z_0 is enough. It means that the full equations including the scaled factor, $l_s = l_{model} / l_{full}$, could be expressed as follows

$$u = \frac{u_*}{\kappa} \ln\left(\frac{z + z_0 * l_s}{z_0 * l_s}\right) \tag{20}$$

$$k = \frac{u_*^2}{\sqrt{C_\mu}} \sqrt{C_1 \cdot \ln\left(\frac{z + z_0 * l_s}{z_0 * l_s}\right) + C_2} \tag{21}$$

$$\omega = \frac{u_*}{\kappa \sqrt{C_\mu}} \frac{1}{z + z_0 * l_s} \tag{22}$$

$$\varepsilon = \frac{u_*^3}{\kappa (z + z_0 * l_s)} \sqrt{C_1 \ln\left(\frac{z + z_0 * l_s}{z_0 * l_s}\right) + C_2} \tag{23}$$

For the "Power-law" type, the mean velocity u and TKE profiles could be scaled as Eqs. (24) and (25) directly, while the expressions of ω and ε need to keep their original form based on their physical meanings. Thereby, the full equations including the scaled factor l_s could be expressed as follows

$$u = u_r \left(\frac{z}{z_r * l_s}\right)^{\alpha_i} \tag{24}$$

$$k = \sqrt{D_1 (z / l_s)^{\alpha_i} + D_2} \tag{25}$$

$$\omega = \frac{\alpha_i}{\sqrt{C_\mu}} \frac{u}{z} \tag{26}$$

$$\varepsilon = \alpha_i C_\mu^{\frac{1}{2}} \frac{u}{z} \sqrt{D_1 z^{\alpha_i} + D_2} \tag{27}$$

It is easy to imagine that if the mean wind velocity u differs from 10 m/s at 10m height, above equations need scaling according to the velocity scale relationship.

6. Conclusions

Modelling an equilibrium atmospheric boundary layer is a basic requirement for computational wind engineering and many efforts had been done in recent years. In this research, two new sets of inflow boundary conditions, i.e., the “Log-law” type and the “Power-law” type, are theoretically presented and numerically verified for the SST k-ω model. Meanwhile, a method of determining the constants in the new models is introduced, and a parameter system corresponding to four typical wind terrains is proposed for general use purpose. The full equations considering the scale effect are presented finally.

The aim of this paper is to providing a concise and consistent way to define the inflow boundary conditions for numerical simulations based on RANS method without introducing relatively complex modification to the turbulence model itself. The efficiency of such method in improving the CFD accuracy of ABL flow had been illustrated by an example of a low-rise building by authors (Yang *et al*. 2008). Nevertheless, more efforts and discussions still need be done to further improve the numerical accuracy closing to the wall as already demonstrated in the paper in the future, mainly through combing with an improved theoretically consistent wall function, which had been already emphasized by previous research.

Acknowledgements

Financial supports of this study from the National Natural Science Foundation of China under Grant Nos. 51478194 and 51178441 and State Key Laboratory of Subtropical Building Science under Grant No. 2017KB14 are gratefully appreciated.

References

Balogh M. and Parente A. (2015), "Realistic boundary conditions for the simulation of atmospheric boundary layer flows using an improved k–ε model", *J. Wind Eng. Ind. Aerod.*, **144**, 183-190.

Barić, E., Džijan, I. and Kozmar, H. (2010), "Numerical simulation of wind characteristics in the wake of a rectangular building submitted to realistic boundary layer conditions", *Transactions of Famena*, **34**(3), 1-10.

Blocken, B., Stathopoulos, T. and Carmeliet, J. (2007), "CFD simulation of the atmospheric boundary layer: wall function problems", *Atmosph. Environ.*, **41**(2), 238-252.

Blocken, B. (2014), "50 years of Computational Wind Engineering: Past, present and future", *J. Wind Eng. Ind. Aerod.*, **129**, 69-102.

Davenport, A.G. (1967), "The dependence of wind loads on meteorological parameters", *Proceedings of the International Seminar on Wind Effects on Buildings and Structures*, Ottawa, Canada.

Eurocode 1: Actions on structures-Part 1-4: General actions-Wind actions. http://eurocodes.jrc.ec.europa.eu/.

Franke, J., Hellsten, A., Schlünzen, H. and Carissimo, B. (2007), "Best Practice Guideline for the CFD Simulation of Flows in the Urban Environment", COST Office, Brussels, ISBN 3-00-018312-4. http://www.mi.uni-hamburg.de/Official-Documents.5849.0.html

Hargreaves, D.M. and Wright. N.G. (2007), "On the use of the k–ε model in commercial CFD software to model the neutral atmospheric boundary layer", *J. Wind Eng. Ind. Aerod.*, **95**(5), 355-369.

Gorlé, C., van Beeck, J. and Rambaud, P. (2010), "Dispersion in the wake of a rectangular building: validation of two reynolds-averaged navier-Stokes modelling approaches", *Bound. –Lay. Meteorol.*, **137** (1), 115-133.

Gorlé, C., van Beeck, J., Rambaud, P. and Van Tendeloo, G. (2009), "CFD modelling of small particle dispersion: The influence of the turbulence kinetic energy in the atmospheric boundary layer", *Atmosph. Environ.*, **43**, 673-681.

Kozmar, H. (2011), "Wind-tunnel simulations of the suburban ABL and comparison with international standards", *Wind Struct.*, **14**(1), 15-34.

Labovský, J. and Jelemenský, L. (2011), "Verification of CFD pollution dispersion modelling based on experimental data", *J. Loss Prevent. Proc.*, **24**(2), 166-177.

Load Code for the Design of Building Structures, GB 5009-2012, Ministry of Construction, China.

Menter, F.R. (1994), "Two-equation eddy-viscosity turbulence models for engineering applications", *AIAA J.*, **32**(8), 1598-1605.

O'Sullivan, J.P., Archer, R.A. and Flay, R.G.J. (2011), "Consistent boundary conditions for flows within the atmospheric boundary layer", *J. Wind Eng. Ind. Aerod.*, **99**, 65-77.

Parente A., Gorlé C., van Beeck J. and Benocci C. (2011a), "Improved k-ε model and wall function formulation for the RANS simulation of ABL flows", *J. Wind Eng. Ind. Aerod.*, **99**, 267–278.

Parente A., Gorlé C., van Beeck J. and Benocci C. (2011b), "A comprehensive modelling approach for the neutral atmospheric boundary layer: Consistent inflow conditions, wall function and turbulence model", *Bound. – Lay.Meteorol.*, **140**, 411-428.

Richards P.J. and Hoxey R.P. (1993), "Appropriate boundary conditions for computational wind engineering models using the k-ε model", *J. Wind Eng. Ind. Aerod.*, **46-47**, 145-153.

Richards, P.J., Quinn, A.D. and Parker, S. (2002), "A 6 m cube in an atmosphere boundary layer flow, Part 2. Computational solutions", *Wind Struct.*, **5**(2-4), 177-192.

Richards, P.J. and Norris, S.E. (2011), "Appropriate boundary conditions for computational wind engineering models revisited", *J. Wind Eng. Ind. Aerod.*, **99**(4), 257-266.

Richards, P.J. and Norris, S.E. (2015), "Appropriate boundary conditions for a pressure driven boundary layer", *J. Wind Eng. Ind. Aerod.*, **142**, 43-52.

Tominaga, Y., Mochida, A., Yoshie, R., Kataoka, H., Nozu, T., Yoshikawa, M. and Shirawasa, T. (2008), "AIJ guidelines for practical applications of CFD to pedestrian wind environment around buildings", *J. Wind Eng. Ind. Aerod.*, **96** (10-11), 1749-1761.

Yang, W. (2004), “Numerical simulation research on the wind loads of building structures and their dynamic responses based on RANS”, Ph.D. Dissertation, Tongji University, Shanghai.

Yang, W., Quan, Y., Jin, X.Y., Tamura, Y. and Gu, M. (2008), “Influences of equilibrium atmosphere boundary layer and turbulence parameter on wind loads of low-rise building”. *J. Wind Eng. Ind. Aerod.*, **96**, 2080-2092.

Yang, Y., Gu, M., Chen, S.Q. and Jin, X.Y. (2009), “New inflow boundary conditions for modeling the neutral equilibrium atmospheric boundary layers in Computational Wind Engineering”, *J. Wind Eng. Ind. Aerod.*, **97**(2), 88-95.

AD